

*Article*

## Optimization Of Hydrocarbon Ejector Using Computational Fluid Dynamics

Muhammad Hadi<sup>1,a</sup>, Ahsan Arshad<sup>1,b</sup>, Nagoor Basha Shaik<sup>2,c,\*</sup>, Watit Benjapolakul<sup>2,d,\*\*</sup>, and Qandeel Fatima Gillani<sup>3,e</sup>

<sup>1</sup> Chemical Engineering Department, NED University of Engineering & Technology, Karachi, Pakistan

<sup>2</sup> Artificial Intelligence, Machine Learning, and Smart Grid Technology Research Unit, Department of Electrical Engineering, Faculty of Engineering, Chulalongkorn University, Bangkok 10330, Thailand

<sup>3</sup> Department of Civil Engineering, COMSATS University, Islamabad, Abbottabad Campus, Abbottabad 22010, Khyber Pakhtunkhwa, Pakistan

E-mail: <sup>a</sup>haadi.engr@gmail.com, <sup>b</sup>ahsanarshad.writer112@gmail.com, <sup>c,\*</sup>nagoor.s@chula.ac.th

(Corresponding author), <sup>d,\*\*</sup>watit.b@chula.ac.th (Corresponding author), <sup>e</sup>qandeelgillani@cuilahore.edu.pk

**Abstract.** Ejector is a powerful emerging thermo-compressor, which is more effective when used with hydrocarbon refrigerants because of its unique thermophysical properties. Therefore, in the present work, a steam ejector model is designed and validated with experimental results to evaluate its accuracy, followed by a detailed comparative study of hydrocarbons and synthetic refrigerants namely pentane, propane, butane, iso-butane, R1234-ze and R1234-yf by computational fluid dynamics and literature Review. The effectiveness of both classes of refrigerants is measured through entrainment ratio, critical backpressure, and thermophysical properties (Literature Review). Pentane was selected as a working fluid since it has comparatively high combination of entrainment ratio and critical back pressure with refrigeration compatible properties. Lastly, the optimized geometry was simulated by varying diameter of constant area zone, nozzle exit position and nozzle expansion angle through Computational Fluid dynamics. The simulation results provide insight into shockwaves, boundary layer separation, vortex formation of ejector flow.

**Keywords:** COP, critical backpressure, entrainment ratio, hydrocarbon refrigerants.

ENGINEERING JOURNAL Volume 26 Issue 5

Received 25 December 2021

Accepted 10 May 2022

Published 31 May 2022

Online at <https://engj.org/>

DOI:10.4186/ej.2022.26.5.1

## Nomenclature & Abbreviation

<i>m</i>	ODP	Ozone Layer Depletion Layer
<i>n</i>	GWP	Global Warming Potential
<i>o</i>	COP	Co-efficient of Performance
<i>p</i>	Nxp	Nozzle Exit Position
<i>q</i>	$\theta$	Angles
<i>r</i>	$\omega$	Entrainment Ratio
<i>s</i>	D	Channel Diameter(m)
<i>t</i>	L	Channel Length(m)
<i>u</i>	ms	Mass of Secondary Stream
<i>v</i>	mp	Mass of Primary Stream

$$\omega = \frac{ms}{mp} \quad (1)$$

## Subscripts

<i>c</i>	diffuser or related
<i>d</i>	mixing area related (CAS or CAC)
<i>e</i>	entrained flow related
<i>w</i>	motive flow related
<i>x</i>	motive nozzle exit
<i>t</i>	motive nozzle of constant area zone or throat
<i>crit</i>	critical state
<i>sat</i>	saturated state

## 1. Introduction

In hot climatic regions, air conditioning systems are the primary source of electricity consumption. It has been reported that in Abu Dhabi, 70% of electricity consumption is due to air conditioning [1]. Modern cooling systems use high global warming potential refrigerants (GWP), which increases carbon footprints [2]. This research work aimed to develop an ejector with fewer carbon footprints according to the United Nations Sustainable Development goals and the Paris Agreement.

Hydrocarbon Ejectors have a broad scope for refrigeration in hot climatic countries [3]. It is due to its unique thermophysical properties and low GWP [4]. Ejectors are thermo-compressors that use high-pressure primary motive flow to induce a low-pressure secondary stream, which is then subjected to mixing, followed by a pressure rise at the outlet of the diffuser. It consists of four components: primary nozzle, mixing chamber, Constant Area Zone or Throat, and Subsonic diffuser, as illustrated in Fig. 1. The nozzle expands the high-pressure primary stream, which creates a vacuum at the nozzle's outlet and entrains the low-pressure secondary stream. Then comes the mixing chamber, whose efficient design and orientation reduce momentum and pressure losses while mixing two fluids. The combined stream undergoes a pressure rise inside the constant area zone, whose improper design may lead to boundary layer separation [5]. A diffuser is used to create a compression effect. This economical compression effect is the reason for the argument for replacing ejectors with power-consuming compressors. There are two main parameters on which the performance of the ejector depends: entrainment ratio ( $\omega$ ) given by (1) and critical backpressure (diffuser outlet pressure) [6].

The coefficient of performance (COP) reflects the energy efficiency of the refrigeration cooling system. COP of the ejector-based refrigeration cycle is directly proportional to the entrainment ratio of an ejector. Hence a high-value entrainment ratio ensures a high value of COP. The ability of hydrocarbon ejectors to use low-grade thermal energy [6], no use of any active part (reduce risk of cavitation) makes refrigeration economical. However still, compressors are dominant because of the low COP values of ejector-driven cycles. Low COPs are because of the poor design of ejectors, operating conditions, and less efficient refrigerants. Many researchers worked on improving ejector design. [7] performed a computational study on the mixing process in a steam ejector using different nozzle structures. [8] and [9] performed parametric studies, including the axial nozzle position to achieve the highest entrainment ratio. [10] and [11] investigated the influence of different configurations of the primary nozzle on ejector performance with fixed geometry for other parts of the ejector. [12] and [13] investigated the influence of the area ratio between the constant area section and the primary nozzle throat and the length of the constant area section. [14] performed numerical simulations to optimize the geometry of the mixing chamber by investigating the effect of the angle of convergence and the diameter of the mixing chamber [15] considered that traditional single-stage ejector-divergent have complex flow conditions such as shock waves, vortexes, shear layers. [14] thought the boundary layer separation hurts the ejector performance and efficiency, as it reduced the entrainment ratio and may lead an external fluid from the condenser to flow back into the ejector. [7] studied the flow irreversibility of R744 ejector by the entropy increase based on CFD simulation. Nutthanun et al. evaluated the theoretical and practical performance of a hybrid compressor and ejector refrigeration system for vehicle air conditioning applications [16]. The suggested mathematical modelling incorporated the 1-dimensional ejector analysis with the thermodynamic analysis of the hybrid compressor and ejector refrigeration system. Utilizing a 24 factorial experimental design, the CFD model was created using the governing equations to explore the influence of crude oil parameters on the transport profile [17]. A high level of agreement between the developed numerical model and commercial software implies that the suggested numerical scheme is appropriate for modelling the transport profile of crude oil through a pipeline and forecasting the phenomena influencing conditions [18]. CFD analysis was applied in several investigations for various scenarios including fluid flows, nano fluid characteristics, and crude oil characteristics [19-21].

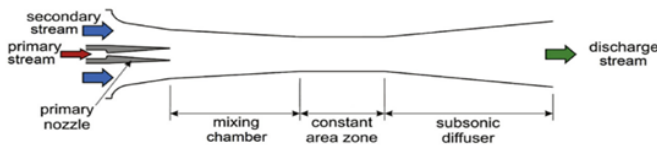


Fig. 1. Illustration of Different Parts of Ejector [22].

Numerous research in recent years have produced many solutions for dealing with various challenges in various contexts. Ping et al. used CFD to evaluate the effect of temperature phase shift on a two-phase ejector. In this work, the transient behavior of a two-phase ejector is simulated in order to determine the ideal operating parameters for greater ejector performance [23]. Saleh et al. used CFD to build high-performance hydrocarbon ejectors for cooling in hot climatic locations. The NIST real gas model is used to accurately forecast ejector performance by including the thermophysical parameters of actual refrigerants [24]. Mustafa et al. constructed a steam ejector utilizing finite volume methods, and the Mach number and pressure in a constant cross-section were compared to analytical data from the literature. In their work, they used ANSYS Fluent to execute numerical computations, and in the turbulent flow, they used energy equations to perform heat transfer-based studies [25]. The CFD model was validated using a steam ejector refrigeration system by Yu Han et al., and the GCI approach was given for assessing grid density [26]. Jakub et al. offered the most extensively used devolatilization, gas-phase, and surface reaction models. They concluded that the heterogeneous and Water-gas-shift reactions had the biggest influence on overall gasification performance and gas-phase modeling, respectively [27]. As a result, high precision necessitates the use of a calibration process or sophisticated models. Parallely, Ruiqing et al. addressed many studies that were systematically grouped to describe their applications of CFD in the research fields of fires, explosions, and hazardous discharge dispersions [28]. Using data from CFD simulations, a quasi-one-dimensional (1D) mathematical model connected with a water ejector is provided by victor et al. They devised a mathematical model to determine the friction loss coefficients of the ejector components, forecast their maximum efficiency point, and define their operating environment [29]. Yafei et al. developed a unique non-equilibrium CFD model to simulate flashing in a CO<sub>2</sub> ejector while taking evaporation and cavitation effects into account [30].

## 2. Methodology

This section details the governing equations used in the study, model description, CFD based ejector design, Geometrical, Physical, & Mesh models, Boundary conditions, and Optimization.

## 2.1. Governing Equations

Since flow inside the ejector is steady, compressible, and turbulent [31], fluid flow Eq. (2)-(5) below are used.

Continuity:

$$\frac{D\rho}{Dt} = \rho \text{div} \quad (2)$$

Momentum:

$$\rho \frac{Du}{Dt} = \rho g - \nabla p + \nabla \tau_{ij} \quad (3)$$

Energy:

$$\rho \frac{Dh}{Dt} = \frac{Dp}{Dt} + \text{div}(k\nabla T) + \tau_{ij} \frac{\partial u_i}{\partial x_j} \quad (4)$$

where the term  $\tau_{ij}$  can be written as:

$$\tau_{ij} = \mu \left( \frac{\partial u_i}{\partial x_j} + \frac{\partial u_j}{\partial x_i} - \frac{2}{3} I \text{div} u \right) \quad (5)$$

where  $I$  is the identity matrix.

## 2.2. Model Description

Using a converging-diverging nozzle, primary high-pressure flow from the generator is converted into a jet of the low-pressure stream with high momentum. This low-pressure stream entrains the secondary stream, which is subjected to mixing and following it a series of normal shock waves [32] and [33], which results in pressure rise. The lift in the diffuser outlet may increase static pressure by compression [34].

## 2.3. CFD Based Ejector Design

Computational fluid dynamics analysis divides the flow domain into a finite set of control volumes. Each control volume has an integral equation which is converted into an algebraic equation. Then each algebraic equation is solved using a numerical method with either a segregated or coupled algorithm [35]. Figure 2 shows the basic parameters and symbols related to the dimensions of the ejector.

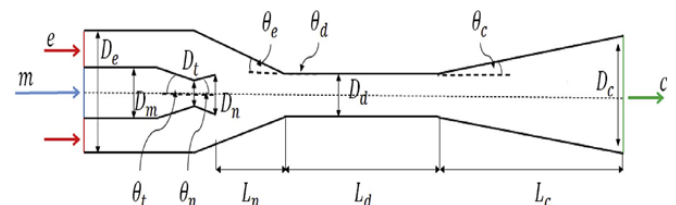


Fig. 2. Basic Ejector's Diagram.

## 2.4. Geometrical Model

To visualize, analyze, and predict fluid flows, certain assumptions are used to analyses hydrocarbon ejectors. Model is designed and tested in ANSYS fluent 20.

Geometry is taken from reference [22] and designed in a design modeler of Ansys fluent. In [36], 2D and 3D models were analyzed using computational fluid dynamics, an advanced computer-based numerical technique, and it was recommended that due to minor variation in results, 2D planar would be a better choice. Similarly, a 2D axisymmetric and planar model were also numerically tested. The variation in results was negligible; hence we selected a 2D axisymmetric model, as shown in Fig. 3, which will ease mesh generation and reduce computational time. The use of an axisymmetric solver indicates the absence of circumferential gradients. Table 1 shows the ejector's dimensions. The materialistic properties of different refrigerants for computation are given in Table 2.

Table 1. Geometric parameters.

Cross-Section		Lengths		Angles	
Parameters	Value (mm)	Parameters	Value (mm)	Parameters	Value (°)
$D_m$	10	$L_n$	155	$\theta_t$	2
$D_t$	3.3	$L_d$	75	$\theta_n$	5
$D_n$	13.6	$L_c$	210	$\theta_e$	4
$D_e$	106			$\theta_c$	2
$D_d$	25.4			$\theta_d$	0.2



Fig. 3. Selected geometry.

Table 2. Materialistic properties of different refrigerants.

Refrigerants	Specific Heat (J/kg-k)	Thermal Conductivity (w/m-k)	Viscosity (kg/m-s)	Molecular Weight (kg/k-mol)
pentane	2436	0.0144	7.20E-06	72.15139
propane	1549	0.0177	7.95E-06	44.09
butane	2620	0.0159	7.00E-06	58.1243
Iso-butane	1632.8	0.0137	6.86E-06	58.1243
R1234 ze	975.8	0.0136	1.22E-05	114.0416
R1234 yf	813.8	0.00928	9.01E-06	114.0416

## 2.5. Physical Model

It was seen that the real gas model was giving results similar to the ideal gas model with a longer convergence time; hence the ideal gas model is selected in the present research [5]. For the selection of turbulence model, simulation is performed using three different models: K-Omega SST, standard k epsilon, and realizable k epsilon (with standard wall function), as shown in Fig. 4. It is found that K-Omega SST gives the slightest deviation of

3.86 % along with the reasonable prediction of shear flow, far wakes, and mixing layers in ejectors flow. So, K-Omega SST is used in this paper. Pressure coupled solver is used in this case, as it is for compressible flows having a high Reynolds number. Flow courant number of 100 is kept in most trials, and relaxation factors of momentum, energy, specific dissipation, turbulent kinetic energy are 0.3,0.5,0.3,0.3 respectively. Pressure inlets and outlets are kept as boundary conditions. Turbulent viscosity ratio and turbulent kinetic energy are kept 10,1 respectively. A second-order discretization scheme is set to discretize all terms. Convergence tolerance of  $1 \times 10^{-6}$  is set for all terms, along with monitor plots of mass imbalance and entrainment ratio.

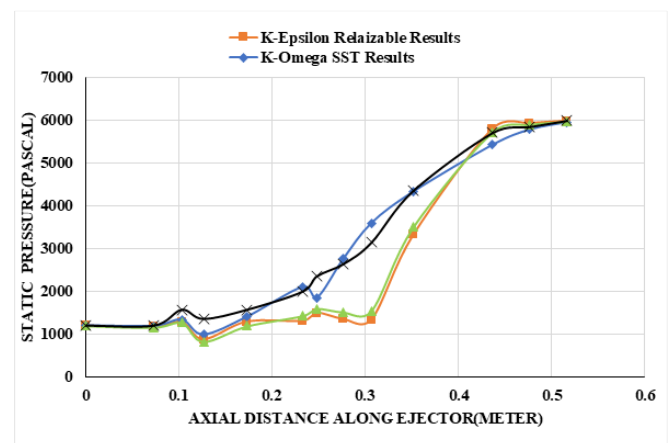


Fig. 4. Comparison of different models.

## 2.6. Boundary Conditions

Dependent variables are specified on the boundaries of the flow domain, which provides a unique solution for a given model. Ejector components include a combination of the nozzle, suction chamber body, constant area section, including diffuser. The compressible flow, in our case, is saturated flow at all boundaries. Table 3 enlists boundary conditions for all simulations performed.

Table 3. Boundary conditions.

Variable	Range
Inlet Primary Pressure	270000 PASCAL
Inlet Secondary Pressure	1200 PASCAL
Outlet Pressure	3000-7500 PASCAL

## 2.7. Mesh Model

An axisymmetric 2D ejector model is meshed using quadrilateral elements. It provides higher orthogonal quality and lowers skewness with fewer cells, leading iteration to reduce convergence tolerance with a more reliable solution, as opposed to triangular mesh. A face sizing function of 0.28 mm is used on nozzle and ejectors throat to resolve steep gradients, whereas 1mm

size cells are used on inlet secondary and diffuser outlet. Then whole geometry is face meshed to reduce skewness. A  $y$  plus of 1.5, which is close to 1, is maintained near-wall through adaptive meshing in fluent. Since K-Omega SST uses near-wall refined mesh treatment instead of wall function approach. Total mesh elements and quality is shown in Table 4. Figures 5 (a) and (b), shown below, depict the mesh domain described above. The solution is discretized on a grid density of 76334 elements, as shown in Fig. 6.



Fig. 5. (a) Optimal grid.

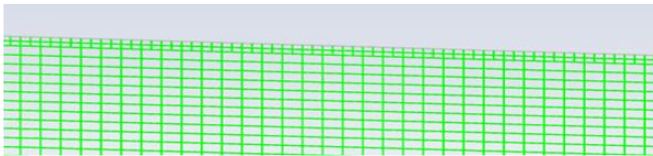


Fig. 5. (b) Near wall.

Table 4. Mesh matrix.

Matric	Value
Orthogonal quality	0.99398
Skewness	0.0384
Aspect ratio	1.6203
Elements	76334

## 2.8. Optimization

Since entrainment ratio and critical back pressure are governing parameters in ejector analysis, a comparative study is conducted between refrigerants based on these two parameters, and the refrigerant found with the better combination is given preference.

## 3. Results and Discussion

### 3.1. Grid Sensitivity Analysis

Next, to find the dependency of entrainment ratio on grid density and find the optimum grid for the model, we carried out a grid sensitivity analysis.

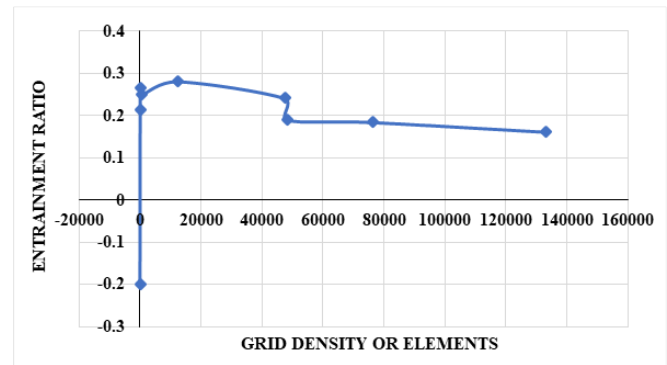


Fig. 6. Grid sensitivity analysis.

From the above Fig. 6, it can be seen that after 76336 elements, the variation in entrainment ratio is less than 3%, which is not a significant deviation; hence it is the optimum grid for the developed model.

### 3.2. Model Validation

Until now, we have discussed selection and reasons for selecting the model and optimal grid size. Now we verify its accuracy by comparing it with experimental results of [22]. All experimental results were generated at their critical mode. Figure 7 shows that the model slightly over-predicts the static pressure at the Constant Area Zone of the ejector using the ideal gas assumption. Secondly, the use of improper sealing of equipment in the experimental investigation may also cause this error. However, the overall simulated results seem to fit over experimental ones with a percentage deviation of 3.82%, which is acceptable. Figure 8 shows the temperature contour of the validated model, where steep temperature gradients are predicted at the diffuser's outlet, indicating the compression effect at the condenser's inlet stream.

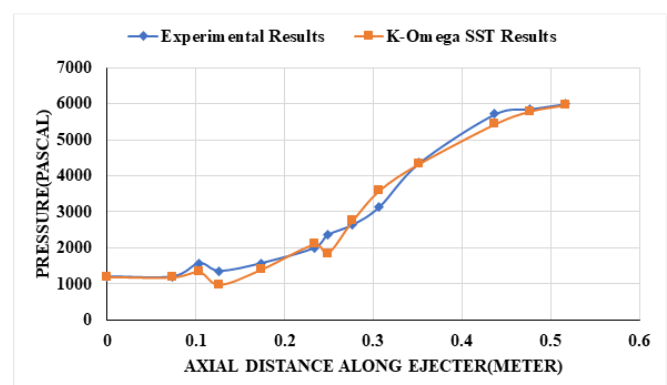


Fig. 7. Validation graph.

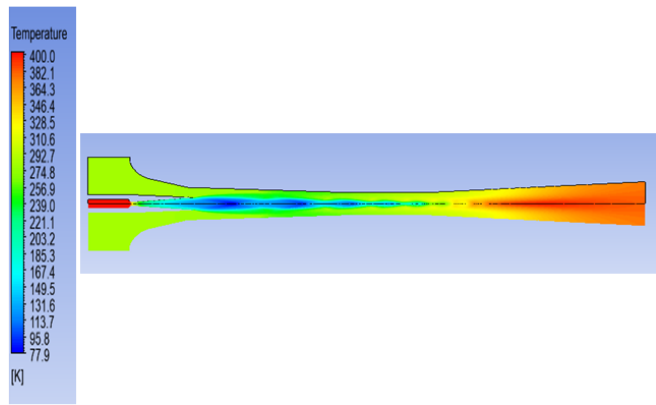


Fig. 8. Temperature contours.

### 3.3. Optimization

#### 3.3.1. Selection of refrigerant

From an industrial point of view, synthetic refrigerants have maintained a high coefficient of performance (COP) in refrigeration cycles. Still, from the environmental sustainability point of view, it has led to increased global warming potential (GWP) and high ozone layer depletion potential (ODP), which increases heat content in the atmosphere and reduces ozone layer thickness due to the presence of chlorine. Therefore, the idea of the revival of hydrocarbon refrigerant has been growing. On the other hand, hydrocarbon refrigerants are environmentally friendly due to low GWP, low ODP, and in addition to that, they are cheap. [12] did a comparative study between synthetic and hydrocarbon refrigerant and proved that the two hydrocarbons, namely pentane and propane, have refrigeration favorable properties like lower operating pressure, higher volumetric capacity, lower kinematic viscosity, lower surface tension, and lower liquid-vapor density ratio in comparison R123Yf, r1234ze at both low and high saturation temperatures. ASHRAE has rated hydrocarbons like isobutane in the "A" category, which is less toxic. However, due to its higher flammability, one should handle it safely, or in other words, strict SOPS should be followed when using it. So, we have seen that from a sustainability point of view, hydrocarbons are more environmentally friendly. The only thing left is to compare both the classes from the entrainment ratio and critical backpressure. Therefore, we simulated both. In Fig. 9 shown below, 270000 pressures at inlet primary and 1200 pressure at inlet secondary are held constant while backpressure is varied up to 7500 pascals. It can be seen that propane has the highest entrainment ratio while pentane has the lowest but has higher critical backpressure. In addition, that pentane is a positive slope refrigerant which means it is not condensation prone and much safer to operate. Therefore, we select pentane for geometric study.

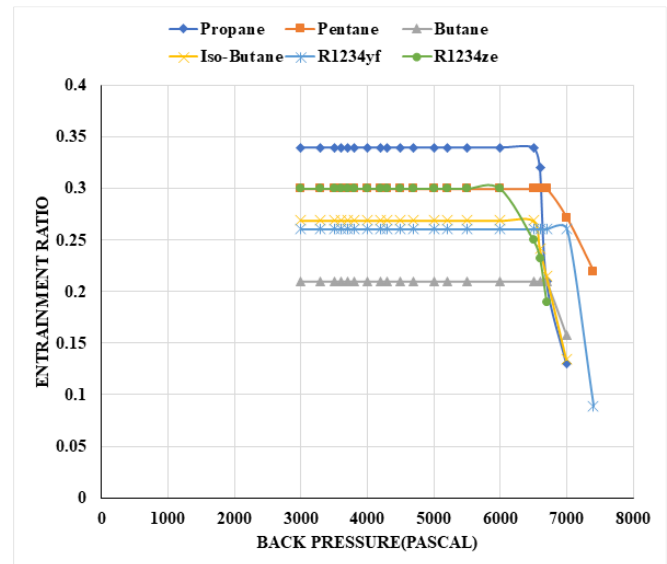


Fig. 9. Graph Of Different Fluids for Entrainment.

Figure 10 shows a plot between static pressure and axial distance. From the graph, propane's maximum entrainment ratio is justified by its low suction pressure at the nozzle's outlet. Even though R1234yf, isobutane, butane has the lowest suction pressure, their entrainment ratio is lower than propane, which means the jet released from the nozzle outlet is overexpanded, decreasing the effective effectiveness area of the constant area zone hence allowing less entrain vapor to pass.

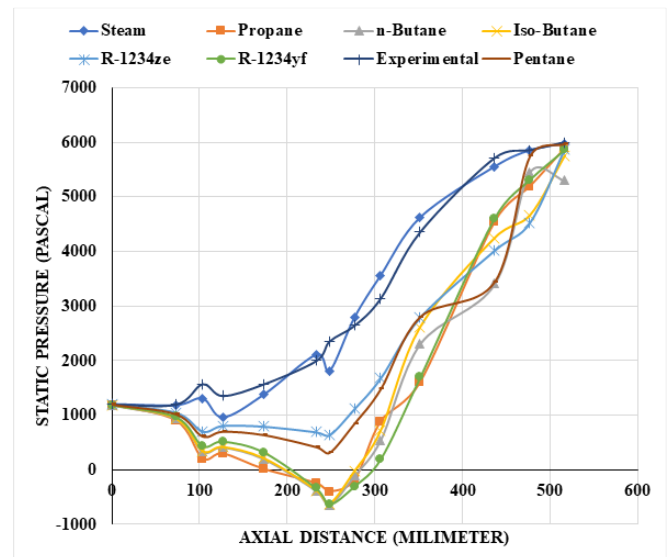


Fig. 10. Graph Of different fluids for static pressure.

Figures 11 and 12 compare the contour plots of pentane and propane. It can be seen in Fig. 12 that the low velocity of the primary fluid at the nozzle outlet causes less momentum transfer between secondary fluid, which leads to less momentum and pressure loss hence producing the most critical back pressure at the diffuser outlet. This justifies higher critical back pressure of pentane in comparison to the low value of propane Fig. 11.

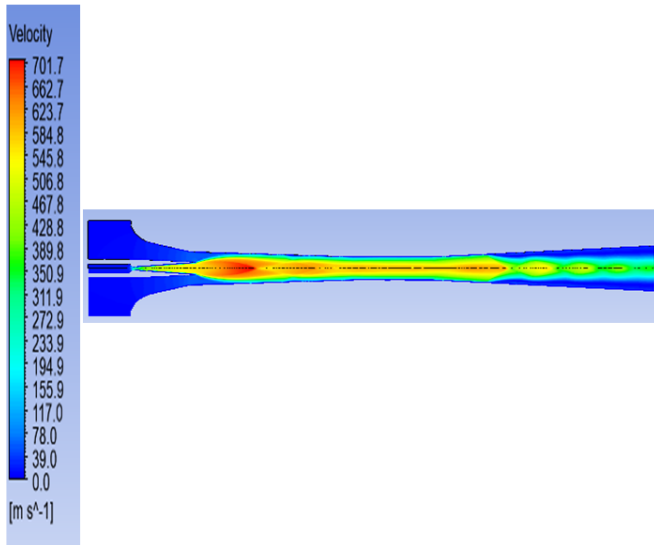


Fig. 11. Propane contour.

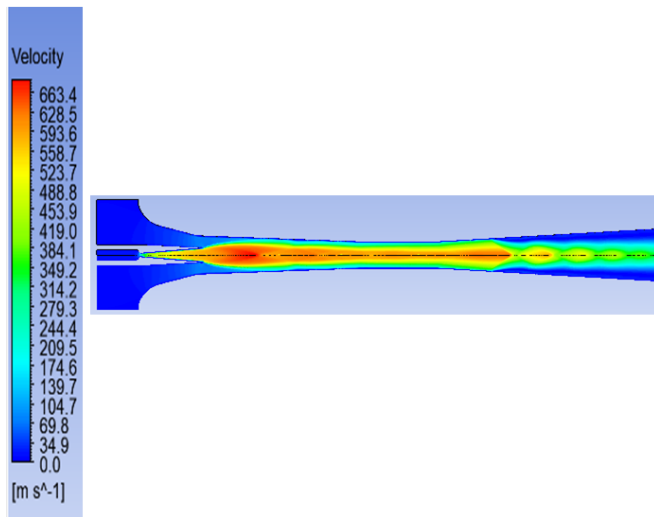


Fig. 12. Pentane contours.

### 3.4. Geometric Analysis

When altering geometry, boundary layer separation was found to impact the entrainment ratio negatively, as studied by [37]. Therefore, we need to find the optimal size of  $N_{xp}$ , the diameter of the constant area zone, expansion angle at which there is no boundary layer separation, and choke flow is maintained. Pentane is used as a working fluid.

#### 3.4.1. Varying diameter of constant area zone

In Fig. 13, we analyze the effect of varying Diameter of Constant Area Zone on entrainment ratio, the diameter sizes of 25,30,40,49,55,65 mm are selected. A numerical analysis was performed on each size, and it was found that the entrainment ratio values are low for smaller values of diameter sizes. This is because the narrow flow passage causes the increase in velocity gradient between the wall and the mixed fluid, which

results in vortex formation and leads to detachment of the boundary layer. The detachment of the boundary layer causes a reduction in the effective area of the constant area zone and decreases the entrainment ratio, as shown in Fig. 14. Further decrease in diameter size may lead to vortex enlargement and further decrement in entrainment ratio.

On the other hand, increasing diameter to 40 mm causes a reduction in vortexes enlargement; hence entrainment ratio increases. At the diameter size of 40 mm in Fig. 14, the entrainment ratio is maximum; therefore, it is the optimal diameter of the constant area zone. On further increasing of diameter, the entrainment ratio again starts to decrease; this is because the mixed fluid near the wall too weak to move is overtaken by inverse pressure gradient produced by backpressure, resulting in the formation of vortexes, which is represented in Fig. 14.

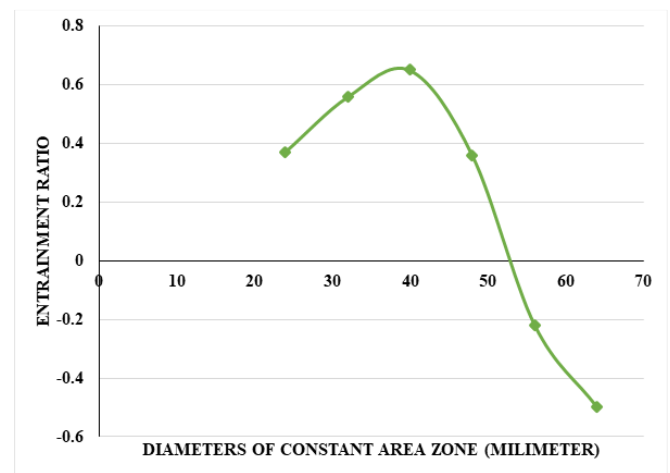


Fig. 13. Diameter Of Constant Area Zone vs. Entrainment Ratio.

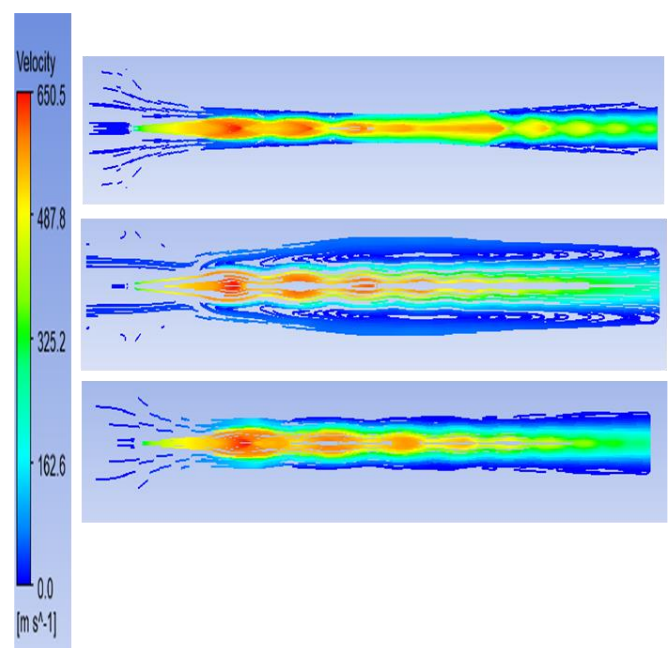


Fig. 14. Vortex formation at 24 mm, 40 mm, and 56mm.

Figure 14 shows vortex formation at different diameters of Constant Area Zone, 24mm, 40mm, and 56mm, respectively.

### 3.4.2. Varying $N_{xp}$

The nozzle position is varied inside the ejector to predict the nozzle exit position ( $N_{xp}$ ) effect on the entrainment ratio. Therefore, simulation is performed on nozzles exit position of -60, -50, -30, -10, 10, 100 mm, shown in Fig. 15. It was seen that on smaller  $N_{xp}$ s, the mixed fluid stream comes into contact with the wall, and this, together with an inverse pressure gradient, leads to the production of vortices, which is a cause of boundary layer separation shown in Fig. 16. Hence entrainment ratio decreases. However, till the  $N_{xp}$ s value of -50 mm, the entrainment ratio increases. There is no boundary layer separation at  $N_{xp}$  value of -50mm, so it has a maximum entrainment ratio. Therefore we declare it as optimal  $N_{xp}$  value Fig. 17. As the  $N_{xp}$  value increases beyond the optimal value, the effective area starts to decrease. The vortex enlargement increases at diffusers outlet, leading to boundary layer separation and reduction in entrainment ratio Fig. 18.

Figure 16 shows vortex formation at different  $N_{xp}$ s of -60mm, -50 mm, and 100 mm, respectively.

### 3.4.3. Varying Expansion Angle

From Fig. 17, there is no such significant impact of varying nozzles expansion angle on entrainment ratio. Still, it can be seen from Fig. 18 that is at an expansion angle value below  $4^\circ$  may cause the primary jet from the nozzle to get weaker; hence the low value of entrainment ratio is witnessed. However, at the expansion angle of  $6^\circ$ , there is strong shockwaves generation from the mixing chamber to the constant area zone, which is the reason for the high entrainment ratio, as shown in Fig. 18. Hence it is our optimal expansion angle; beyond that point, the variation in expansion angle is not significant to be neglected. The streamline flow shown below indicates that when optimum expansion angle is maintained, then despite adverse pressure gradient, the choke flow is dominant.

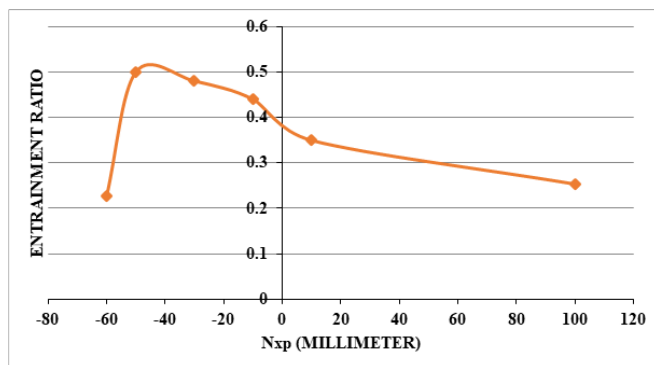


Fig. 15.  $N_{xp}$  vs. Entrainment Ratio.

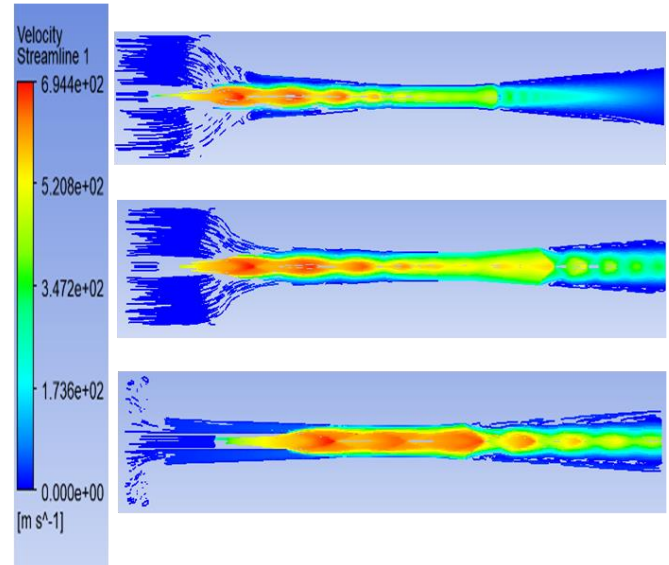


Fig. 16. Vortex Formation At -60 mm, -50 mm and 100mm.

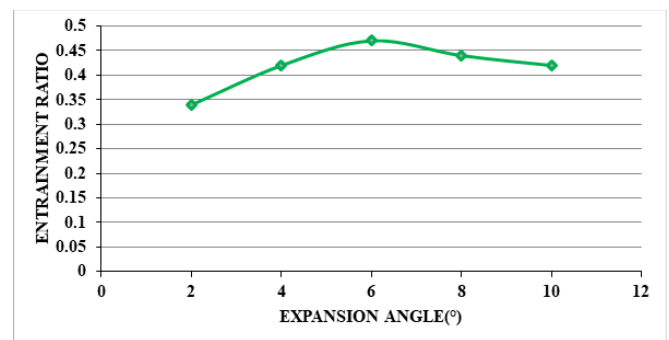


Fig. 17. Expansion Angle vs. Entrainment Ratio.

Figure 18 shows vortex formation at different nozzle expansion angles of  $2^\circ$  and  $6^\circ$ , respectively.

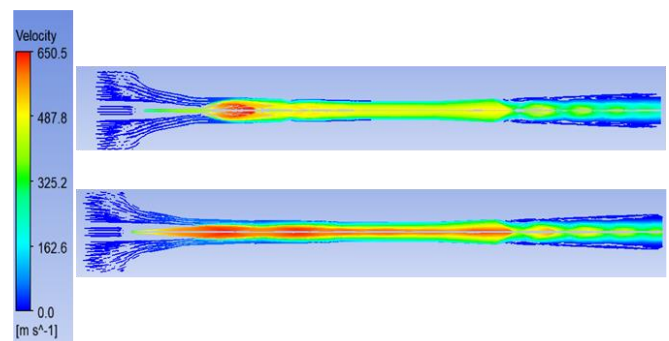


Fig. 18. Vortex Formation at  $2^\circ$  and  $6^\circ$ .

## 4. Conclusions

In this research work, the study is conducted on the merits and demerits of using synthetic and hydrocarbon refrigerant and the criterion for refrigeration selection using literature and computational fluid dynamics.



Furthermore, a parametric study was performed by varying design parameters such as ejector's Nxp, the diameter of constant area zone, and expansion angle to see the effect on entrainment ratio. Moreover, we noticed an optimum value of each design parameter, after which the entrainment ratio goes to a declining trend. Following are some conclusions that are drawn from this study:

- Synthetic refrigerants are not only expensive but also become the reason for high global warming potential. The CFD results of this work show that pentane outperformed synthetic refrigerants as per their lower entrainment ratio and critical backpressure. Also, pentane and other hydrocarbons are relatively cheaper than synthetic refrigerants.
- Lesser diameter of constant area zone causes a reduction in the effective area, while the larger diameter of constant area zone may lead to the weakening of shockwaves which causes back pressure propagation and hence reduction in entrainment ratio.
- The ideal flow pattern can be achieved with even lesser energy loss by obtaining the sustainable low GWP refrigerant and a decent combination of entrainment and critical back pressure and optimal geometry.

## Acknowledgment

The authors are thankful to NED University and Chulalongkorn University for the facilities provided during the research conducted.

## References

- [1] S. Mohamed, A. Al Masabai, Y. Shatilla, and T. Zhang, "Design of high-performance refrigerant ejector for sub-ambient cooling," in *2016 15th IEEE Intersociety Conference on Thermal and Thermomechanical Phenomena in Electronic Systems (ITherm)*, 2016, pp. 1458-1465.
- [2] B. Bakthavatchalam, N. B. Shaik, and P. B. Hussain, "An artificial intelligence approach to predict the thermophysical properties of MWCNT nanofluids," *Processes*, vol. 8, no. 6, p. 693, 2020.
- [3] X. Chen, S. Omer, M. Worall, and S. Riffat, "Recent developments in ejector refrigeration technologies," *Renewable and Sustainable Energy Reviews*, vol. 19, pp. 629-651, 2013.
- [4] T. Zhang and S. Mohamed, "Conceptual design and analysis of hydrocarbon-based solar thermal power and ejector cooling systems in hot climates," *Journal of Solar Energy Engineering*, vol. 137, no. 2, p. 021001, 2015.
- [5] Y. Han, X. Wang, H. Sun, G. Zhang, L. Guo, and J. Tu, "CFD simulation on the boundary layer separation in the steam ejector and its influence on the pumping performance," *Energy*, vol. 167, pp. 469-483, 2019.
- [6] S. Mohamed, Y. Shatilla, and T. Zhang, "CFD-based design and simulation of hydrocarbon ejector for cooling," *Energy*, vol. 167, pp. 346-358, 2019.
- [7] K. Banasiak et al., "A CFD-based investigation of the energy performance of two-phase R744 ejectors to recover the expansion work in refrigeration systems: An irreversibility analysis," *International Journal of Refrigeration*, vol. 40, pp. 328-337, 2014.
- [8] P. Desevaux, A. Mellal, and Y. Alves de Sousa, "Visualization of secondary flow choking phenomena in a supersonic air ejector," *Journal of Visualization*, vol. 7, no. 3, pp. 249-256, 2004.
- [9] K. Matsuo, Y. Miyazato, and H.-D. Kim, "Shock train and pseudo-shock phenomena in internal gas flows," *Progress in Aerospace Sciences*, vol. 35, no. 1, pp. 33-100, 1999.
- [10] S. B. Riffat and S. Omer, "CFD modelling and experimental investigation of an ejector refrigeration system using methanol as the working fluid," *International Journal of Energy Research*, vol. 25, no. 2, pp. 115-128, 2001.
- [11] S. Varga, A. C. Oliveira, and B. Diaconu, "Numerical assessment of steam ejector efficiencies using CFD," *International Journal of Refrigeration*, vol. 32, no. 6, pp. 1203-1211, 2009.
- [12] X. Yang, X. Long, and X. Yao, "Numerical investigation on the mixing process in a steam ejector with different nozzle structures," *International Journal of Thermal Sciences*, vol. 56, pp. 95-106, 2012.
- [13] W. Fu, Y. Li, Z. Liu, H. Wu, and T. Wu, "Numerical study for the influences of primary nozzle on steam ejector performance," *Applied Thermal Engineering*, vol. 106, pp. 1148-1156, 2016.
- [14] Y. Bartosiewicz, Z. Aidoun, P. Desevaux, and Y. Mercadier, "Numerical and experimental investigations on supersonic ejectors," *International Journal of Heat and Fluid Flow*, vol. 26, no. 1, pp. 56-70, 2005.
- [15] F. Kong and H. Kim, "Analytical and computational studies on the performance of a two-stage ejector-diffuser system," *International Journal of Heat and Mass Transfer*, vol. 85, pp. 71-87, 2015.
- [16] N. Keerlatiyadatanapat, T. Sriveerakul, N. Suvarnakuta, and K. Piantong, "Experimental and theoretical investigation of a hybrid compressor and ejector refrigeration system for automotive air conditioning application," *Engineering Journal*, vol. 21, no. 5, pp. 105-123, 2017.
- [17] W. Rukthong, P. Piumsomboon, W. Weerapakkaron, and B. Chalermssinsuwan, "Computational fluid dynamics simulation of a crude oil transport pipeline: Effect of crude oil properties," *Engineering Journal*, vol. 20, no. 3, pp. 145-154, 2016.
- [18] N. B. Shaik, S. R. Pedapati, A. Othman, K. Bingi, and F. A. Abd Dzubir, "An intelligent model to predict the life condition of crude oil pipelines using artificial neural networks," *Neural Computing*

- and Applications, vol. 33, no. 21, pp. 14771-14792, 2021.
- [19] P. Chaiwang, B. Chalermssinsuwan, and P. Piumsomboon, "Two-dimensional CFD simulation of reducing operating pressure effect on the system hydrodynamics in a downer reactor," *Engineering Journal*, vol. 21, no. 2, pp. 133-149, 2017.
- [20] N. Kardan, H. Hakimzadeh, and Y. Hassanzadeh, "Investigation of the dynamics bed shear stress distribution around a circular cylinder using various turbulences models," *Engineering Journal*, vol. 21, no. 7, pp. 75-86, 2017.
- [21] F. Ismail, A. Rashid, and M. Mahbub, "CFD analysis for optimum thermal design of carbon nanotube based micro-channel heatsink," *Engineering Journal*, vol. 15, no. 4, pp. 11-22, 2011.
- [22] K. Ariafar, D. Buttsworth, G. Al-Doori, and N. Sharifi, "Mixing layer effects on the entrainment ratio in steam ejectors through ideal gas computational simulations," *Energy*, vol. 95, pp. 380-392, 2016.
- [23] P. Zheng, B. Li, and J. J. E. Qin, "CFD simulation of two-phase ejector performance influenced by different operation conditions," *Energy*, vol. 155, pp. 1129-1145, 2018.
- [24] S. Mohamed, Y. Shatilla, and T. Zhang, "CFD-based design and simulation of hydrocarbon ejector for cooling," *Energy*, vol. 167, pp. 346-358, 2019.
- [25] M. Atmaca and C. Ezgi, "Three-dimensional CFD modeling of a steam ejector," *Energy Sources, Part A: Recovery, Utilization, Environmental Effects*, vol. 44, no. 1, pp. 2236-2247, 2022.
- [26] Y. Han, X. Wang, H. Sun, G. Zhang, L. Guo, and J. Tu, "CFD simulation on the boundary layer separation in the steam ejector and its influence on the pumping performance," *Energy*, vol. 167, pp. 469-483, 2019.
- [27] J. Mularski, H. Pawlak-Kruczek, and N. Modlinski, "A review of recent studies of the CFD modelling of coal gasification in entrained flow gasifiers, covering devolatilization, gas-phase reactions, surface reactions, models and kinetics," *Fuel*, vol. 271, p. 117620, 2020.
- [28] R. Shen, Z. Jiao, T. Parker, Y. Sun, and Q. Wang, "Recent application of Computational Fluid Dynamics (CFD) in process safety and loss prevention: A review," *Journal of Loss Prevention in the Process Industries*, vol. 67, p. 104252, 2020.
- [29] V. J. de Oliveira Marum et al., "Performance analysis of a water ejector using Computational Fluid Dynamics (CFD) simulations and mathematical modeling," *Energy*, vol. 220, p. 119779, 2021.
- [30] [30] Y. Li and J. J. E. Deng, "Numerical investigation on the performance of transcritical CO<sub>2</sub> two-phase ejector with a novel non-equilibrium CFD model," *Energy*, vol. 238, p. 121995, 2022.
- [31] S. Varga, A. C. Oliveira, and B. Diaconu, "Influence of geometrical factors on steam ejector performance—A numerical assessment," *International Journal of Refrigeration*, vol. 32, no. 7, pp. 1694-1701, 2009.
- [32] T. Sriveerakul, S. Aphornratana, and K. Chunnanond, "Performance prediction of steam ejector using computational fluid dynamics: Part 2. Flow structure of a steam ejector influenced by operating pressures and geometries," *International Journal of Thermal Sciences*, vol. 46, no. 8, pp. 823-833, 2007.
- [33] K. Yang, H. Lee, and H. Jung, "Numerical prediction of jet behavior of thermal vapor compressor," *Desalination and Water Treatment*, vol. 33, no. 1-3, pp. 248-254, 2011.
- [34] C. Lin, W. Cai, Y. Li, J. Yan, and Y. Hu, "The characteristics of pressure recovery in an adjustable ejector multi-evaporator refrigeration system," *Energy*, vol. 46, no. 1, pp. 148-155, 2012.
- [35] H. K. Versteeg and W. Malalasekera, *An Introduction to Computational Fluid Dynamics: The Finite Volume Method*. Pearson Education, 2007.
- [36] K. Pianthong, W. Seehanam, M. Behnia, T. Sriveerakul, and S. Aphornratana, "Investigation and improvement of ejector refrigeration system using computational fluid dynamics technique," *Energy Conversion and Management*, vol. 48, no. 9, pp. 2556-2564, 2007.
- [37] Y. Bartosiewicz, Z. Aidoun, and Y. Mercadier, "Numerical assessment of ejector operation for refrigeration applications based on CFD," *Applied Thermal Engineering*, vol. 26, no. 5-6, pp. 604-612, 2006.



**Muhammad Hadi** was born in Faisalabad, Pakistan in 29 June 1999. He recently completed his BE Chemical engineering from NED University in 2021. During his Bachelors's study, he developed the design of an adiabatic reactor to study the kinetics of hydrogen peroxide decomposition. He also served as an intern engineer in the Pakistan council of scientific and industrial research in 2019 to extract protein from banana peel. In 2021 his ambition towards solving critical problems brought his attention to the ineffective design of hydrocarbon ejector which is a cheap consumer of electricity and a better alternative to High Carbon footprint producing compressors. He found during his research that the poor design of ejectors leads to low cop. Therefore, he carried out a numerical simulation to bring forward its three alternative designs leading to much higher cops together with environmentally friendly refrigerants.



**Ahsan Arshad** was born in Karachi, Pakistan on 2 January 1998. He completed his BE Chemical engineering from NED University in 2021. During his Bachelors's study, he did the manual design of an adiabatic reactor to make it energy efficient. He also served as an intern engineer in the Pakistan council of scientific and industrial research in 2019 to develop organic products. Apart from them, he is servicing in making and publishing content for articles on the limitations of synthetic refrigerant on various online and offline platforms. In 2021 his ambition towards solving critical problems brought his attention to the ineffective design of hydrocarbon ejector which is a cheap consumer of electricity and a better alternative to High Carbon footprint producing compressors. He found during his research that the poor design of ejectors leads to low cop. Therefore, he carried out a numerical simulation to bring forward its three alternative designs leading to much higher cops together with environmentally friendly refrigerants.



**Nagoor Basha Shaik** is a Post-Doctoral Researcher in AI and ML research unit, Faculty of Engineering, from Chulalongkorn University. He did his Ph.D. in the department of Mechanical Engineering from Universiti Teknologi PETRONAS, Malaysia. He finished his M. Tech in the department of Mechanical Engineering (Specialised in Machine Design) from Jawaharlal Nehru Technological University, Kakinada, India in 2016. He completed his Bachelor of Technology in Mechanical Engineering from Acharya Nagarjuna University, Guntur, A.P in 2011. He worked as a mechanical engineer in India from July 2011- Nov 2014 in India. He published more than 17 articles in good impact factor journals. His area of interest includes materials, artificial intelligence, oil and gas pipelines, piping systems, prediction techniques, manufacturing process, engineering drawing and material properties.



**Watit Benjapolakul** received the D.Eng. degree in electrical engineering from The University of Tokyo, in 1989. He is currently a Professor with the Department of Electrical Engineering, Chulalongkorn University, Thailand. He is also the Head of the Artificial Intelligence, Machine Learning, and Smart Grid Technology Research Unit, Faculty of Engineering, Chulalongkorn University. His current research interests include mobile communication systems, broadband networks, applications of artificial intelligence in communication systems, wireless networks, and applications of communication networks in smart grids.



**Qandeel Fatima Gillani** is born in Pakistan in 1988 . She has earned her BS degree form COMSATS University Islamabad, Lahore Campus in 2009 in Chemical Engineering. She started her career as Lab Engineering in same department. Later, she received her MS degree in Chemical Engineering from Punjab University Lahore Pakistan. After that, she secured a Lecturer position in Chemical Engineering Department of COMSATS University Islamabad, Lahore campus. In 2014, she moved to Malaysia and started job in Mechanical Engineering Department of Univeristi Teknologi Petronas as Graduate Assistance. She has published more than ten articles in good impact factor journals. Her research interest includes Fire retardant materials, Advance materials and nanofillers. Currently she is working as senior lecturer in COMSATS University Islamabad Abbottabad Campus. Qandeel is also a recipient of silver medal in the International Invention, Innovation & Technology Exhibition (ITEX) in 2017 held in Malaysia and best present award in The International Conference on Mechanical, Manufacturing and Process Plant Engineering (ICMMPE 2017).